2026 IEEE/SICE International Symposium on System Integration (SII)
January 11-14, 2026. Cancún, México

Wearable Microblower System for Affective Touch: Airflow-Based Tactile Stroking Stimulation

Youchan Yim[1] and Fumihide Tanaka[2]

***Abstract*— Interpersonal tactile interaction plays a crucial role in emotional regulation and physiological responses, with affective touch demonstrating significant benefits in stress reduction and affective modulation. Existing approaches to replicating affective touch have relied on manual stroking or robotic brushing mechanisms, both of which present limitations in consistency, precision, and real-world applicability. This study introduces a Wearable Microblower System that utilizes airflow-based tactile stimulation to provide precisely controlled and reproducible affective touch stimuli. The system is designed to generate affective touch by producing stroking sensations at CT-optimal velocities and pressures, ensuring effective activation of CT afferents. A systematic performance evaluation confirmed that the device delivers tactile forces within the CT-optimal range, suggesting its potential feasibility for affective haptic applications. Moreover, the proposed system enables continuous and natural stroking through a control strategy that incorporates sequential activation of multiple stroking points. Our evaluation results indicate that the proposed device offers a quantifiable and reproducible means of delivering affective touch, with potential applications in stress alleviation, affective computing, and virtual reality–mediated haptic experiences. Future work will explore empirical validation through comparative studies and further integration with immersive technologies.**

Fig. 1. Design concept: (**a**) and fabricated prototype, (**b**) of the proposed Wearable Microblower System.

I. Introduction

Physical contact between individuals extends beyond mere tactile stimulation, inducing emotional stability and physiological changes [1]–[4]. For instance, physical interaction between parents and children provides emotional comfort, increases oxytocin secretion, and reduces cortisol levels, thereby contributing to stress alleviation [1], [5]–[7]. Additionally, holding hands with an attachment partner has been shown to synchronize heart rate, respiration, and brain activity, while also exerting pain-relieving effects [8]–[11].

Among various forms of physical contact, C-tactile (CT) optimal touch is a specific type of affective touch characterized by gentle stroking at an optimal velocity and pressure range. This touch is known to optimally activate CT afferents, which respond to stroking at velocities between 1 and 10 cm/s with an applied force between 0.3 and 2.5 mN [12]–[15]. The most effective stimulation parameters have been reported as approximately 3 cm/s velocity [12], [16]–[18].

CT afferents are predominantly found in hairy skin regions [19], [20] and are functionally connected to neural circuits involved in emotional processing [13]. Consequently, CT-optimal touch enhances emotional well-being and modulates neurochemical release, increasing levels of neurotransmitters such as oxytocin and serotonin [21]–[25].

Furthermore, CT-optimal touch activates the insular cortex, a brain region rich in opioid receptors associated with both pain modulation and emotional processing. This interaction with the endogenous opioid system contributes to the pleasantness of tactile stimuli and plays a role in pain reduction [26]–[28]. Prior research investigating the effects of affective tactile stimulation has typically employed stroking with a brush applied to the forearm, a region rich in CT afferents.

However, existing studies have employed two primary methods for delivering CT-optimal touch: **manual stroking**, administered by trained experimenters [27]–[32], and **mechanized brushing**, where a robotic apparatus equipped with a brush moves in a pendulum-like motion to simulate stroking [12], [30], [31], [33]–[35]. Comparative studies suggest that both methods yield similar levels of CT afferent

*This work was supported by JSPS KAKENHI Grant Number 24K21320, 25K24420 and JST SPRING Grant Number JPMJSP2124.

[1]Youchan Yim is with Institute of Systems and Information Engineering, University of Tsukuba, Japan yim@ftl.iit.tsukuba.ac.jp

[2]Fumihide Tanaka is with Institute of Systems and Information Engineering, University of Tsukuba, Japan fumihide.tanaka@gmail.com

activation, indicating that the perception of CT-optimal touch may rely more on the tactile properties of the stimulus itself than on its social context [36].

Despite these findings, existing approaches present several limitations. Manual stimulation introduces inter-experimenter variability, leading to inconsistencies in stroking pressure, velocity, and duration. In contrast, mechanized brushing provides greater control over stroking parameters, but lacks adaptability in dynamic, real-world contexts where users may move freely.

To address these challenges, the present study developed a wearable device designed to deliver precisely controlled and consistent CT-optimal touch via uniform tactile stimulation on the skin surface (Fig. 1). This device utilizes Microblowers, allowing for accurate regulation of stroking velocity and applied force. By implementing this system, the study aims to overcome reproducibility issues in previous research, providing a quantifiable and controlled method for investigating CT-optimal touch.

II. Related Work

A. Wearable Stroking Devices

Various wearable devices have been developed to technologically reproduce affective touch, particularly CT-optimal touch. These devices aim to replicate stroking sensations at controlled velocities and pressures, directly interacting with the user's skin.

Several approaches have been proposed to implement stroking haptic feedback in wearable form. One method utilizes pneumatic textile structures to generate tactile stimuli through air pressure modulation [37]. This approach employs mechanically controlled knitted fibers to exert pressure on the skin. However, the method is structurally limited in its ability to simulate continuous stroking, a fundamental characteristic of CT-optimal touch.

Another approach involves linear actuators arranged in a matrix configuration to exert localized pressure on the skin, creating a sensation of movement [38]. While this system can generate various tactile pressure patterns, it struggles to precisely control both velocity and applied force, and its contact area remains limited.

One of the most direct attempts to replicate CT-optimal touch employed a wearable device that performed gentle brush stroking along the forearm [39]. This system applied 3 cm/s stroking on hairy skin regions to examine its impact on anxiety reduction. However, it required constant skin contact, and while the stroking velocity was adjustable, precise force modulation remained a challenge. Additionally, the motorized system posed limitations in size and weight, making integration into everyday wear impractical.

To address these structural limitations, researchers have explored mid-air haptic techniques, where tactile stimuli are delivered without direct skin contact [40]. This method regulates airflow pressure and thermal stimulation, expanding the range of haptic experiences. However, mid-air approaches have inherent technological constraints, which are discussed in the following section.

B. Mid-Air Haptic Devices

Mid-air haptic feedback technology enables tactile stimulation without direct skin contact, often utilizing ultrasound haptic feedback to create localized pressure sensations [41], [42]. A major limitation of ultrasound-based haptics is its reliance on a fixed spatial configuration, requiring the user to remain within a precise distance from the emitter. This significantly limits wearability and mobility. Moreover, while effective for precise point-based pressure feedback, these systems struggle to produce natural stroking sensations across a broad area. While these mid-air haptic techniques offer non-contact feedback, their spatial resolution and directional control remain insufficient for delivering the precise tangential forces required for CT-optimal stimulation. CT afferents are particularly sensitive to gentle, continuous stroking at low force levels across the skin, a requirement that mid-air approaches cannot reliably satisfy. Although recent studies have demonstrated visually plausible simulations of fur stroking using mid-air ultrasound haptics [42], there is still no viable solution for delivering CT-optimal touch in a measurable, lightweight, and untethered form, thereby indicating the current gap between mid-air haptic capabilities and affective touch requirements.

Another related approach in mid-air haptics involves synthetic air-jet systems, where controlled bursts of air reproduce tactile sensations on the skin [43]. Although not directly investigating the effects related to CT afferent activation, previous research has combined DC fans with Peltier modules to realize direct airflow stimulation accompanied by thermal variations [40]. However, user feedback revealed that airflow-based haptics were often perceived as mere wind exposure rather than genuine stroking sensations. Furthermore, the bulkiness of the system hindered its feasibility as a wearable device. Compared to ultrasound-based haptics, this approach is more hardware-efficient, yet research on its real-world application remains limited, and the need for additional space for airflow regulation complicates wearable integration.

Although direct air stimulation on the skin has traditionally been considered ineffective in activating CT afferents [16], recent findings suggest that hair movements induced by air puffs are strongly coupled with CT afferent activity, increasing the potential for reproducing CT-optimal touch through direct air puffs [44]. Therefore, this study aims to quantitatively reproduce continuous low-force tactile input to deliver gentle stroking forces and to address the common limitations of prior mid-air haptic studies through wearable integration.

III. Device Development and Implementation

A. Development Objectives and Approach

This study aims to develop a Wearable Microblower System (Fig. 2) capable of delivering consistent and quantifiable tactile stroking stimuli, addressing the limitations of previous methods used to implement CT-optimal touch. While prior approaches have attempted to replicate affective touch through mechanical actuators or mid-air haptics, these

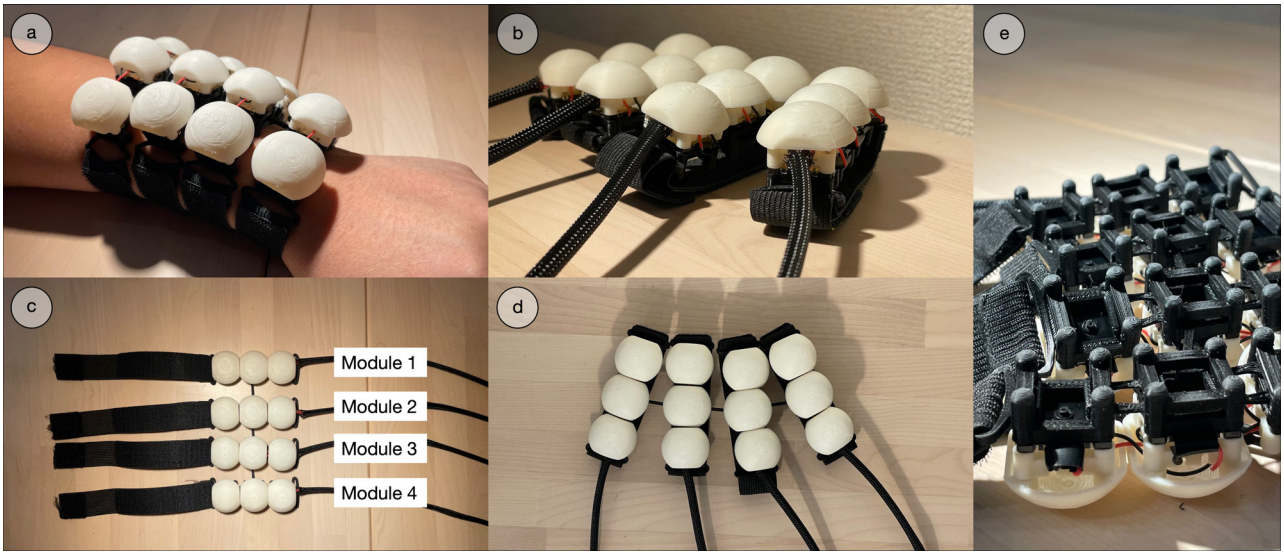

Fig. 2. Detailed views of the prototype: (**a**) Prototype mounted on the left forearm, (**b**)(**c**)(**d**) Individual stroking tactile points, (**e**) Skin-contacting surface of the prototype (rear view). The microcontroller and battery circuits for driving each module are not shown in the figure but are also mounted on the forearm.

methods have struggled with limitations in precise control over velocity and pressure, as well as adaptability in real-world conditions. To overcome these challenges, the present study employs a Microblower-based system (MZB1001T02, Murata, Japan), which generates precise airflow-based tactile stimulation without requiring direct mechanical contact with the skin. This approach offers several advantages over conventional methods, including a broader stimulation area, smoother stroking motion, and enhanced portability as a wearable system.

B. Hardware Design

The configuration of the Wearable Microblower System prototype is shown in Fig. 3. For circuitry and control, each stroking tactile point was connected to a dedicated driver circuit (MZBD002, Murata, Japan), with three Microblowers per driver. To achieve a realistic stroking sensation, the device was designed to incorporate multiple stroking tactile points, each composed of three Microblowers arranged in a linear formation. A total of four driver circuits (four stroking tactile points) were integrated into the system, and each tactile point was sequentially activated by controlling the ON/OFF switching of the applied voltage through an external power supply and an Arduino Mega microcontroller. The system regulates the voltage supplied to each driver using either a MOSFET-based circuit or a discharge-capable configuration employing DPDT relays and a coil driver, enabling the generation of continuous airflow motion across the skin surface.

The spacing between individual Microblowers was determined based on the two-point discrimination (TPD) threshold for the human arm and forearm, which has been reported to range between 30.7 mm and 45.4 mm [45]. To prevent the perception of discrete pressure points rather than continuous stroking, the spacing between the three Microblowers within a single stroking tactile point module was set to 26.7 mm, ensuring that the airflow would be interpreted as a unified stroking sensation rather than isolated point stimuli. Considering the diffusion characteristics of airflow upon skin contact, the actual perceived stimulation area may be smaller than the designed spacing. The device consists of four stroking points and utilizes a total of 12 Microblowers. The spacing between stroking points can be maintained at a maximum of 39.2 mm, ensuring that it falls within the threshold of TPD. This design was implemented to facilitate the natural perception of sequential stroking.

For wearability and comfort, the device was designed to maintain a consistent distance between the Microblowers and the skin while minimizing physical contact with the body. To achieve this, a structural support bridge was incorporated to hold the Microblower modules at a fixed elevation. These components were fabricated using soft thermoplastic elastomer (TPE) filaments with a hardness rating of 60A (TPE60A, HottyPolymer), ensuring a flexible yet stable structure. The contact points between the device and the skin were designed with a hemispherical profile to minimize skin irritation and discomfort. Additionally, the inter-module connections were fabricated using TPE60A to allow for natural flexion and conformation to the curvature of the forearm, further enhancing wearability and adaptability. To secure the device, elastic bands were integrated on both sides, ensuring stable attachment while accommodating a range of forearm sizes. The structural components of the device were 3D printed using PLA and ABS materials with Raise3D Pro3 and Stratasys F120 printers. For enhanced durability, metal shafts measuring 1.5 mm in diameter and 20 mm in length were used to connect individual parts.

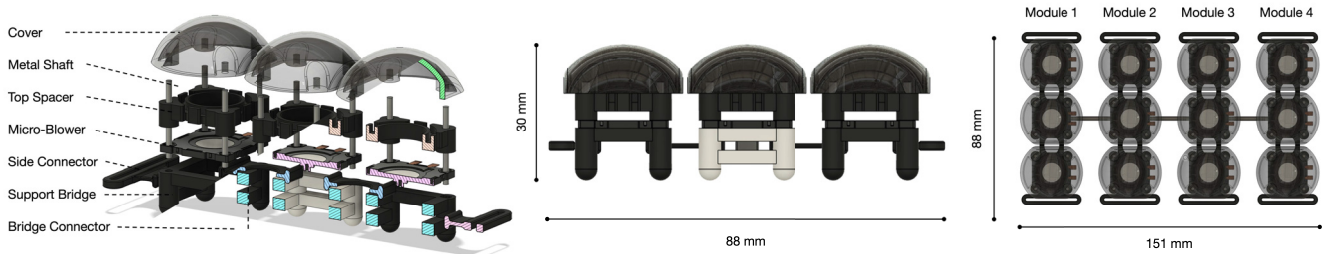

Fig. 3. 3D model of the developed Wearable Microblower System. The components include: Cover (ABS) for structural protection, Top Spacer (PLA) for air intake and wire management, Microblower (MZB1001T02) for airflow-based tactile stimulation, Support Bridge (TPE) to maintain a 0.010 m air outlet distance, Metal Shaft for structural stability, Bridge Connector (TPE) for flexible module linking, and Side Connector (TPE) for securing the device with Velcro straps.

C. Control Strategy for Smooth Stroking Tactile Stimulation

To achieve a smooth and continuous stroking sensation, it is crucial to design an activation pattern that prevents users from perceiving discrete pressure points. The developed device consists of four stroking tactile point modules arranged linearly, with an inter-module spacing of 39.2 mm. If the modules were activated sequentially without overlapping, the stimulation would exhibit noticeable discontinuities, reducing the effectiveness of the stroking effect. To mitigate this issue, a partially overlapping activation strategy is employed to create a seamless transition between modules.

Given the desired stroking velocity of 3 cm/s (30 mm/s, CT-optimal touch), the activation time for each module can be determined as follows:

$$t_{\text{single}} = \frac{\text{Inter-module Distance}}{\text{Stroking Velocity}} = \frac{39.2 \text{ mm}}{30 \text{ mm/s}} \approx 1.31 \text{ s} \quad (1)$$

Thus, each module must remain activated for approximately 1.31 seconds to ensure that the perceived stroking motion matches the intended speed.

To further enhance the smoothness of the stroking effect, the transition between modules is optimized by introducing a temporal overlap in the activation sequence. Instead of turning off one module before activating the next, the adjacent module is gradually turned on while the preceding module remains active for a short duration. This overlapping time is set to 50% of the activation period, ensuring that the perceived tactile stimulation blends seamlessly.

The overlap duration is given by:

$$t_{\text{overlap}} = 0.5 \times t_{\text{single}} = 0.66 \text{ s} \quad (2)$$

This means that after a module is activated, the subsequent module turns on 0.66 seconds later, and the preceding module turns off only after an additional 0.66 seconds. This approach ensures that at any given moment, at least two adjacent modules are active, generating a more fluid and continuous tactile experience. Based on the calculated activation times, the optimized ON/OFF sequence for the four stroking tactile point modules is outlined in Fig. 4.

This pattern ensures that at least two modules are active simultaneously during each transition, creating a gradual tactile shift that mimics the sensation of continuous stroking rather than a sequence of discrete pressure points.

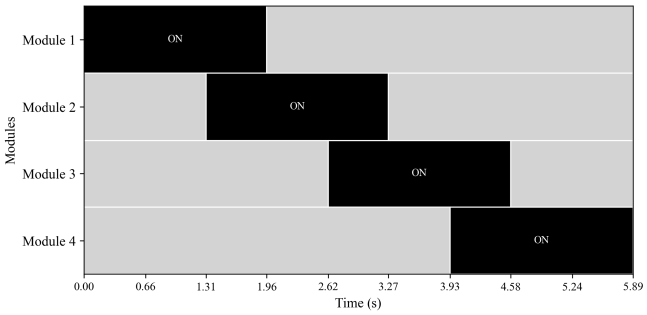

Fig. 4. Optimized activation sequence for continuous stroking tactile stimulation. Each horizontal band represents the activation state of a Microblower module over time. Black regions indicate ON periods, while gray regions indicate OFF periods. Overlapping ON durations between adjacent modules correspond to transitional airflow, enabling a continuous stroking sensation.

IV. Evaluation of Output Characteristics

Technical Specifications of the Microblower

The Microblower used in this study measures 20 × 20 mm, with a thickness of 3.45 mm and a protrusion height of 1.6 mm, ensuring minimal bulk for integration into wearable applications. The Microblower is driven by a dedicated control circuit, with an adjustable operating voltage ranging from 11.5 V to 21 V, allowing for modulation of the airflow intensity. According to the manufacturer's datasheet, under maximum voltage conditions (21 Vdc), the device delivers an unloaded airflow rate of 1.2 L/min, while at 16.5 Vdc it delivers 0.95 L/min, and at 11.5 Vdc, it delivers 0.6 L/min. The air exits through a circular outlet with a diameter of 2 mm, and the resulting airflow characteristics depend on the applied voltage.

Estimation of Airflow Expansion at 0.010 m Distance

As air is expelled from the Microblower through a circular outlet of diameter D_{outlet}, it expands in a conical shape following a typical axial jet flow pattern. This expansion can be characterized by a divergence angle θ, which defines the angular spread of the jet. The diameter of the jet at a distance

d from the outlet, denoted as D_{expanded}, can be determined by using the following geometric equation (Fig. 5(c)):

$$D_{\text{expanded}} = D_{\text{outlet}} + 2\tan(\theta) \times d \tag{3}$$

By substituting $D_{\text{outlet}} = 0.002$ m, $\theta = 7.5°$, and $d = 0.010$ m, the expanded diameter of the jet is calculated as:

$$\begin{aligned} D_{\text{expanded}} &= 0.002 + 2 \cdot \tan(7.5°) \cdot 0.010 \\ &= 0.00463 \text{ m} \end{aligned} \tag{4}$$

This corresponds to an expanded area calculated as:

$$\begin{aligned} A &= \pi \left(\frac{D_{\text{expanded}}}{2} \right)^2 \\ &= \pi \left(\frac{0.00463}{2} \right)^2 = 1.683 \times 10^{-5} \text{ m}^2 \end{aligned} \tag{5}$$

The choice of 7.5 °for θ is based on empirical observations from airflow studies, where low-pressure laminar jets tend to diverge within the 5°–10° range depending on environmental conditions [46], [47]. This assumption provides a reasonable approximation in the absence of precise divergence measurements.

The selection of $d = 0.010$ m was based on empirical evaluation of the current prototype. Through preliminary testing, it was observed that at shorter distances (e.g., $d = 0.005$ m), the airflow sometimes made direct contact with the skin, which is undesirable for consistent mid-air haptic presentation. Conversely, distances greater than 0.02 m caused the airflow to disperse too widely, failing to recreate the desired localized stroking sensation. Therefore, a distance of 0.010 m was adopted as a practical compromise in the current prototype. In future iterations, the optimal distance will be identified through further theoretical modeling and empirical force measurements.

Calculation of Force Applied to the Skin at 0.010 m Distance

To estimate the force exerted by the airflow on the skin surface, we use the dynamic pressure equation, as shown below:

$$F = \frac{1}{2}\rho v^2 A \tag{6}$$

where: F is the force (N) applied to the skin, ρ is the air density (1.225 kg/m³), v is the air velocity (m/s) at 0.010 m distance, A is the expanded airflow area (1.683×10^{-5} m^2).

To determine the force applied to the skin surface using the given equation, we measured the maximum airflow velocity at a distance of 0.010 m from the Microblower's air outlet, as illustrated in Fig. 5. The measurement was conducted using a thermo anemometer (TESTO 405-V1, TESTO, Germany). The results of airflow velocity measurements corresponding to the input voltage (Vdc) supplied to the driving circuit are presented in Fig. 6. Based on the previously obtained expanded area results, the force at a 0.010 m distance for each applied voltage was calculated and summarized in

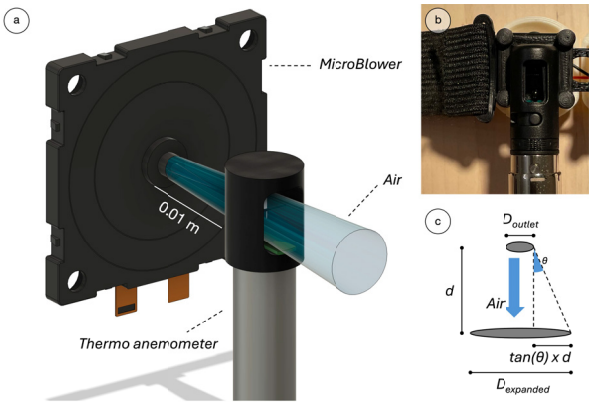

Fig. 5. (**a**) Illustration depicting the measurement process using a thermo-anemometer positioned 10 mm from the Microblower outlet. (**b**) Close-up view of the actual measurement setup with the Microblower module and measuring device. (**c**) Diagram illustrating the geometric estimation of the expanded air jet area based on the divergence angle and distance from the outlet.

TABLE I
FORCE EXERTED ON THE SKIN AT 0.010 M DISTANCE.

Voltage (Vdc)	Velocity at 0.010 m (m/s)	Force (mN)
12	4.68 ± 0.27	0.23
14	5.92 ± 0.11	0.36
16	7.16 ± 0.08	0.53
18	8.40 ± 0.12	0.73
20	9.64 ± 0.19	0.96

Table I. Measured results indicated that the applied force exceeded the activation threshold of CT afferents (0.3–2.5 mN [12]–[15]) when the driving voltage ranged from 14 to 20 Vdc.

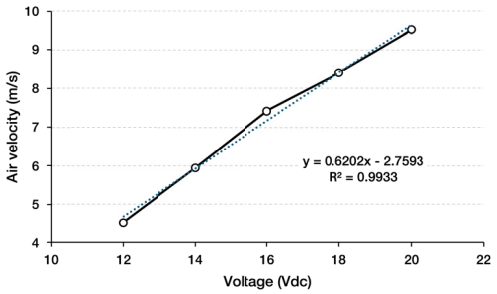

Fig. 6. Relationship between air velocity and driving voltage of the Microblower. Measurements were averaged over three trials per Microblower under ambient conditions (23.8 °C, 61% RH).

V. EXPERIMENTAL EVALUATION OF AIRFLOW FORCE AND PERCEPTUAL RESPONSES

To experimentally evaluate the divergence characteristics of the airflow generated by the Microblower, we investigated the actual divergence angle of the airflow produced by the Microblower using a fog machine with a mixture of 80% vegetable glycerin and 20% propylene glycol. The

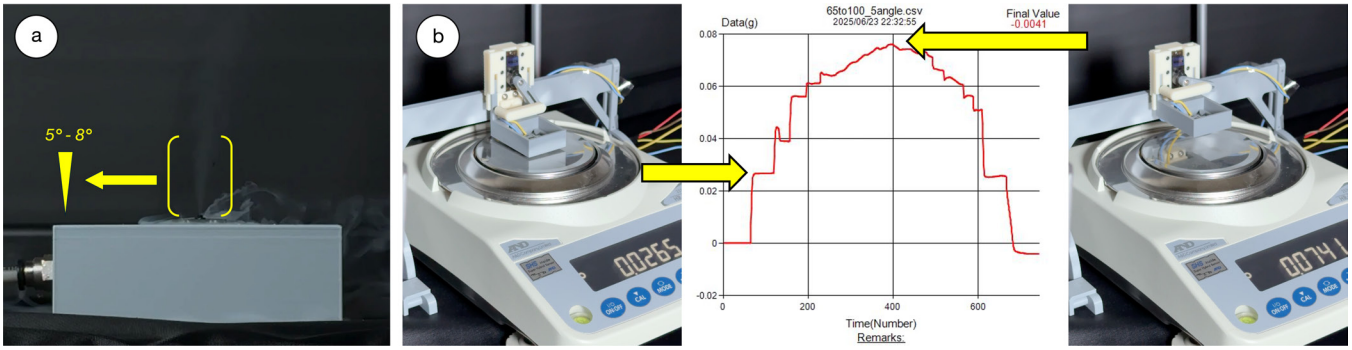

Fig. 7. (**a**) Visualization of airflow divergence using fog (80% vegetable glycerin and 20% propylene glycol), recorded at 4K 120 fps. The flow transitions to turbulence around 15 mm from the outlet, with the divergence angle measured between 5° and 8°. (**b**) Force output of the Microblower measured using an electronic balance (HR250-AZ, A&D, Japan). The airflow exerted 0.26–0.73 mN within a 0–10 mm range at 20 V, corresponding to 0.0265–0.0741 g.

emitted fog was recorded using a 4K camera at 120 fps to visualize the spread of airflow and identify the transition point from laminar to turbulent flow (see Fig. 7(a)). The analysis revealed that the flow transitioned to turbulence at approximately 15 mm from the outlet, with a measured divergence angle ranging between 5° and 8° within the laminar region.

To verify whether the theoretically estimated force values were physically realized, we empirically measured the output force using a precision electronic balance (HR250-AZ, A&D, Japan). When 20 V was applied, the airflow exerted forces ranging from 0.26 mN to 0.73 mN (corresponding to 0.0265 g to 0.0741 g) within a 0–10 mm distance from the outlet (see Fig. 7(b)).

Due to the instability of the ON/OFF driving characteristics of the Microblower circuit at the current development stage, direct perceptual testing using the Microblower array was not feasible. For this reason, the perceptual evaluation reported in this paper was conducted using an air pump configured to match the airflow output characteristics of the Microblower. This test was part of a pilot study that compared air-based stroking with other tactile stroking methods in a separate project. The study protocol was approved by the Research Ethics Committee of the Faculty of Engineering, Information, and Systems at the University of Tsukuba (2025R033).

A total of 4 participants (male = 2; age = 26.750 ± 3.304 years) took part in this preliminary test. Each participant received tactile stimuli generated by the proposed stroking mechanism on the left (non-dominant) forearm, using the parameter settings specified in this study. The perceptual evaluation included one experimental factor, which was a comparison among three stroking velocities: 3 cm/s (CT-optimal touch) and 10 cm/s and 30 cm/s (both CT-non-optimal control conditions). For each condition, the stimulation consisted of five back-and-forth stroking cycles. After each session, participants rated their subjective experience using a 7-point Likert scale on the following aspects: (1) perceived velocity of stroking, (2) continuity, (3) linearity, and (4) pleasantness. As this was a small-scale pilot test, no statistical analysis was conducted due to the limited sample size.

As shown in Fig. 8, perceived velocity ratings clearly differentiated the intended stroking speed across the three conditions, confirming that the stimuli were presented as designed. Continuity ratings were slightly lower in the 30 cm/s condition, whereas linearity remained consistently high across all conditions. Although the sample size was insufficient for statistical testing, the 3 cm/s (CT-optimal) condition yielded the highest mean pleasantness rating.

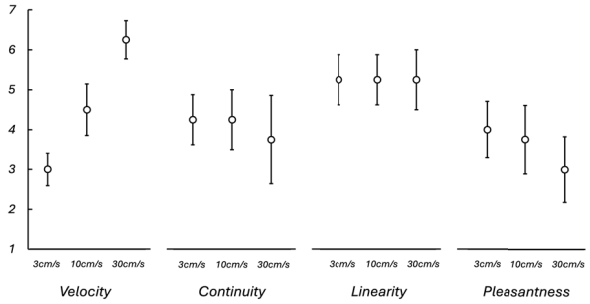

Fig. 8. Mean ratings with SEM across four perceptual measures. The corresponding overlap durations between adjacent modules were 653 ms (3 cm/s), 196 ms (10 cm/s), and 65 ms (30 cm/s).

VI. Conclusions

The airflow-based tactile stroking system proposed in this study is designed to present affective touch, delivering tactile stimuli close to the CT afferent activation threshold (below 1 mN) while providing adjustable and consistent pressure regardless of the geometry of the contact surface. An additional benefit of this system is its generalizability, not only to the upper arm, but also in other regions of hairy skin across the body where CT afferents are distributed [19], [20], without requiring changes to the device configuration.

Previous research has identified a stroking velocity of approximately 3 cm/s as optimal for activating CT afferents [12], [16]–[18], but the force parameter used in these studies was generally adopted without clear empirical justification. Even the foundational study that first proposed this optimal speed [12] employed 0.2 N and 0.4 N without clarifying the rationale, and subsequent studies have continued to

use a fixed force of 0.4 N without further analysis. Although some studies have quantified variable force (200–300 mN) using load cells in robotic brushing setups [48], [49], most have relied on manual stroking by experimenters [27]–[32]. As a result, the force parameter for reliably eliciting CT afferent responses has not yet been empirically established. In this context, the present study contributes to foundational development by enabling quantitative experimentation on the effects of CT-optimal touch.

The system still has several limitations. First, the divergence angle of 7.5° used in the calculation was an assumed parameter and represents a conservative estimate, as it was not directly measured but introduced to simplify the analytical model. In practice, the actual contact area may differ since the experimentally observed divergence angle ranged between 5° and 8° as shown in Fig. 7(a). However, due to the hygroscopic nature of the fog mixture used for visualization, it was difficult to obtain a consistent divergence angle across trials. In future experiments, the contact area could be more accurately visualized by directing the airflow onto fine particles such as sand or powder, while the stimulation force could be measured by placing a load cell beneath a substrate covered with these particles under the same test conditions.

Second, due to the limited output of the current Microblower, higher forces cannot be delivered. As shown in Fig. 7(b), the measurement was conducted by directing the airflow onto the full surface of a metal weighing pan rather than onto human skin, and thus the perceived tactile sensation may differ under actual skin-contact conditions. Although the measured force values are close to the reported threshold for CT afferent activation, they do not necessarily guarantee consistent CT fiber firing. Therefore, it is desirable to enhance the system so that it can reliably generate stimuli both below and above the CT activation threshold. Recent findings [44] revealed that hair movements induced by brief air-puff stimulation are strongly coupled with CT afferent activity, suggesting that airflow-induced tactile cues may engage CT fibers under certain conditions. However, the airflow intensity used in that study was not quantitatively characterized, making it difficult to precisely evaluate the stimulation parameters. Building upon these findings, our future work aims to quantitatively control air-puff stimulation while directly recording CT afferent activity, thereby enabling a more systematic evaluation of air-based stroking systems.

Third, although the spacing between air outlets and between stroking modules was designed with reference to the TPD threshold [45], the system has not yet been evaluated for whether stimuli are perceived as single or multiple points, nor has the continuity of multi-point stimulation been assessed [50]. The pilot experiment conducted in this study served as an initial attempt to investigate the feasibility of the proposed system, and the results indicated that the airflow stimulation was perceived as a gentle stroking sensation. Although the perceptual test was conducted using an air pump rather than the Microblower array, the airflow parameters were matched to the measured Microblower output characteristics; therefore, the pilot study serves to validate the perceptual plausibility of the stroking design rather than the hardware implementation itself. Building on these findings, future studies will examine TPD characteristics of air-jet stimulation to provide a more detailed understanding of its tactile presentation properties.

Future development will aim to overcome these limitations through refined prototypes, followed by user studies to examine the efficacy of CT-optimal touch delivered by the proposed system. In addition, we aim to construct a quantitative dataset of CT afferent responses not only in the upper arm but across the entire body. Furthermore, future work will focus on stabilizing the Microblower driving circuitry to enable fully wearable operation, after which a series of application-oriented user studies will be conducted to evaluate the system's practical effectiveness in diverse contexts.

ACKNOWLEDGMENT

This work was supported by JSPS KAKENHI Grant Number 24K21320, 25K24420 and JST SPRING Grant Number JPMJSP2124.

REFERENCES

[1] T. Field, "Touch for socioemotional and physical well-being: A review," *Developmental Review*, vol. 30, no. 4, pp. 367–383, Dec. 2010.

[2] C. J. Cascio, D. Moore, and F. McGlone, "Social touch and human development," *Developmental Cognitive Neuroscience*, vol. 35, pp. 5–11, Feb. 2019.

[3] I. Morrison, L. S. Löken, and H. Olausson, "The skin as a social organ," *Experimental Brain Research*, vol. 204, no. 3, pp. 305–314, July 2010.

[4] S. Cohen, D. Janicki-Deverts, R. B. Turner, and W. J. Doyle, "Does Hugging Provide Stress-Buffering Social Support? A Study of Susceptibility to Upper Respiratory Infection and Illness," *Psychological Science*, vol. 26, no. 2, pp. 135–147, Feb. 2015.

[5] N. Scatliffe, S. Casavant, D. Vittner, and X. Cong, "Oxytocin and early parent-infant interactions: A systematic review," *International Journal of Nursing Sciences*, vol. 6, no. 4, pp. 445–453, Oct. 2019.

[6] D. Vittner, J. McGrath, J. Robinson, G. Lawhon, R. Cusson, L. Eisenfeld, S. Walsh, E. Young, and X. Cong, "Increase in Oxytocin From Skin-to-Skin Contact Enhances Development of Parent–Infant Relationship," *Biological Research For Nursing*, vol. 20, no. 1, pp. 54–62, Jan. 2018.

[7] A. R. Morris, A. Turner, C. H. Gilbertson, G. Corner, A. J. Mendez, and D. E. Saxbe, "Physical touch during father-infant interactions is associated with paternal oxytocin levels," *Infant Behavior and Development*, vol. 64, p. 101613, Aug. 2021.

[8] P. Goldstein, S. G. Shamay-Tsoory, S. Yellinek, and I. Weissman-Fogel, "Empathy Predicts an Experimental Pain Reduction During Touch," *The Journal of Pain*, vol. 17, no. 10, pp. 1049–1057, Oct. 2016.

[9] P. Goldstein, I. Weissman-Fogel, and S. G. Shamay-Tsoory, "The role of touch in regulating inter-partner physiological coupling during empathy for pain," *Scientific Reports*, vol. 7, no. 1, p. 3252, June 2017.

[10] P. Goldstein, I. Weissman-Fogel, G. Dumas, and S. G. Shamay-Tsoory, "Brain-to-brain coupling during handholding is associated with pain reduction," *Proceedings of the National Academy of Sciences*, vol. 115, no. 11, Mar. 2018.

[11] L. Peled-Avron, P. Goldstein, S. Yellinek, I. Weissman-Fogel, and S. Shamay-Tsoory, "Empathy during consoling touch is modulated by mu-rhythm: An EEG study," *Neuropsychologia*, vol. 116, pp. 68–74, July 2018.

[12] L. S. Löken, J. Wessberg, I. Morrison, F. McGlone, and H. Olausson, "Coding of pleasant touch by unmyelinated afferents in humans," *Nature Neuroscience*, vol. 12, no. 5, pp. 547–548, May 2009.

[13] H. Olausson, J. Wessberg, I. Morrison, F. McGlone, and Å. Vallbo, "The neurophysiology of unmyelinated tactile afferents," *Neuroscience & Biobehavioral Reviews*, vol. 34, no. 2, pp. 185–191, Feb. 2010.

[14] Å. B. Vallbo, H. Olausson, and J. Wessberg, "Unmyelinated Afferents Constitute a Second System Coding Tactile Stimuli of the Human Hairy Skin," *Journal of Neurophysiology*, vol. 81, no. 6, pp. 2753–2763, June 1999.

[15] J. Cole, M. C. Bushnell, F. McGlone, M. Elam, Y. Lamarre, Å. Vallbo, and H. Olausson, "Unmyelinated tactile afferents underpin detection of low-force monofilaments," *Muscle & Nerve*, vol. 34, no. 1, pp. 105–107, 2006.

[16] R. Ackerley, H. B. Wasling, J. Liljencrantz, H. Olausson, R. D. Johnson, and J. Wessberg, "Human C-Tactile Afferents Are Tuned to the Temperature of a Skin-Stroking Caress," *Journal of Neuroscience*, vol. 34, no. 8, pp. 2879–2883, Feb. 2014.

[17] C. Triscoli, H. Olausson, U. Sailer, H. Ignell, and I. Croy, "Ct-optimized skin stroking delivered by hand or robot is comparable," *Frontiers in Behavioral Neuroscience*, vol. 7, no. 208, 2013.

[18] R. Ackerley, I. Carlsson, H. Wester, H. Olausson, and H. Backlund Wasling, "Touch perceptions across skin sites: differences between sensitivity, direction discrimination and pleasantness," *Frontiers in Behavioral Neuroscience*, vol. 8, no. 54, 2014.

[19] H. Olausson, J. Cole, K. Rylander, F. McGlone, Y. Lamarre, B. G. Wallin, H. Krämer, J. Wessberg, M. Elam, M. C. Bushnell, and Å. Vallbo, "Functional role of unmyelinated tactile afferents in human hairy skin: Sympathetic response and perceptual localization," *Experimental Brain Research*, vol. 184, no. 1, pp. 135–140, Jan. 2008.

[20] F. McGlone, J. Wessberg, and H. Olausson, "Discriminative and Affective Touch: Sensing and Feeling," *Neuron*, vol. 82, no. 4, pp. 737–755, May 2014.

[21] S. C. Walker, P. D. Trotter, W. T. Swaney, A. Marshall, and F. P. Mcglone, "C-tactile afferents: Cutaneous mediators of oxytocin release during affiliative tactile interactions?" *Neuropeptides*, vol. 64, pp. 27–38, Aug. 2017.

[22] A. K. Bershad, L. M. Mayo, K. Van Hedger, F. McGlone, S. C. Walker, and H. de Wit, "Effects of MDMA on attention to positive social cues and pleasantness of affective touch," *Neuropsychopharmacology*, vol. 44, no. 10, pp. 1698–1705, Sept. 2019.

[23] P. D. Trotter, F. McGlone, S. McKie, M. McFarquhar, R. Elliott, S. C. Walker, and J. F. W. Deakin, "Effects of acute tryptophan depletion on central processing of CT-targeted and discriminatory touch in humans," *European Journal of Neuroscience*, vol. 44, no. 4, pp. 2072–2083, 2016.

[24] K. Uvnäs-Moberg, "Oxytocin may mediate the benefits of positive social interaction and emotions," *Psychoneuroendocrinology*, vol. 23, no. 8, pp. 819–835, Nov. 1998.

[25] S. C. Walker and F. P. McGlone, "The social brain: Neurobiological basis of affiliative behaviours and psychological well-being," *Neuropeptides*, vol. 47, no. 6, pp. 379–393, Dec. 2013.

[26] L. K. Case, M. Čeko, J. L. Gracely, E. A. Richards, H. Olausson, and M. C. Bushnell, "Touch Perception Altered by Chronic Pain and by Opioid Blockade," *eNeuro*, vol. 3, no. 1, Jan. 2016.

[27] L. L. Meijer, W. Baars, H. Chris Dijkerman, C. Ruis, and M. J. Van Der Smagt, "Spatial factors influencing the pain-ameliorating effect of CT-optimal touch: A comparative study for modulating temporal summation of second pain," *Scientific Reports*, vol. 14, no. 1, p. 2626, Feb. 2024.

[28] M. Von Mohr, C. Krahé, B. Beck, and A. Fotopoulou, "The social buffering of pain by affective touch: A laser-evoked potential study in romantic couples," *Social Cognitive and Affective Neuroscience*, Sept. 2018.

[29] H. W. Olausson, J. Cole, Å. Vallbo, F. McGlone, M. Elam, H. H. Krämer, K. Rylander, J. Wessberg, and M. C. Bushnell, "Unmyelinated tactile afferents have opposite effects on insular and somatosensory cortical processing," *Neuroscience Letters*, vol. 436, no. 2, pp. 128–132, May 2008.

[30] L. S. Löken, M. Evert, and J. Wessberg, "Pleasantness of touch in human glabrous and hairy skin: Order effects on affective ratings," *Brain Research*, vol. 1417, pp. 9–15, Oct. 2011.

[31] I. Morrison, L. S. Löken, J. Minde, J. Wessberg, I. Perini, I. Nennesmo, and H. Olausson, "Reduced C-afferent fibre density affects perceived pleasantness and empathy for touch," *Brain*, vol. 134, no. 4, pp. 1116–1126, Apr. 2011.

[32] R. Ackerley, E. Hassan, A. Curran, J. Wessberg, H. Olausson, and F. McGlone, "An fMRI study on cortical responses during active self-touch and passive touch from others," *Frontiers in Behavioral Neuroscience*, vol. 6, Aug. 2012.

[33] S.-J. Blakemore, C. D. Frith, and D. M. Wolpert, "Spatio-Temporal Prediction Modulates the Perception of Self-Produced Stimuli," *Journal of Cognitive Neuroscience*, vol. 11, no. 5, pp. 551–559, Sept. 1999.

[34] H. Olausson, Y. Lamarre, H. Backlund, C. Morin, B. G. Wallin, G. Starck, S. Ekholm, I. Strigo, K. Worsley, Å. B. Vallbo, and M. C. Bushnell, "Unmyelinated tactile afferents signal touch and project to insular cortex," *Nature Neuroscience*, vol. 5, no. 9, pp. 900–904, Sept. 2002.

[35] F. McGlone, H. Olausson, J. A. Boyle, M. Jones-Gotman, C. Dancer, S. Guest, and G. Essick, "Touching and feeling: Differences in pleasant touch processing between glabrous and hairy skin in humans," *European Journal of Neuroscience*, vol. 35, no. 11, pp. 1782–1788, 2012.

[36] C. Triscoli, H. Olausson, U. Sailer, H. Ignell, and I. Croy, "CT-optimized skin stroking delivered by hand or robot is comparable," *Frontiers in Behavioral Neuroscience*, vol. 7, Dec. 2013.

[37] C. du Pasquier, L. Tessmer, I. Scholl, L. Tilton, T. Chen, S. Tibbits, and A. Okamura, "Haptiknit: Distributed stiffness knitting for wearable haptics," *Science Robotics*, vol. 9, no. 97, p. eado3887, Dec. 2024.

[38] N. Ferguson, M. E. Cansev, A. Dwivedi, and P. Beckerle, "Design of a Wearable Haptic Device to Mediate Affective Touch with a Matrix of Linear Actuators," in *Advances in System-Integrated Intelligence*, M. Valle, D. Lehmhus, C. Gianoglio, E. Ragusa, L. Seminara, S. Bosse, A. Ibrahim, and K.-D. Thoben, Eds. Cham: Springer International Publishing, 2023, pp. 507–517.

[39] Y. Zhao, Y. Tao, G. Le, R. Maki, A. Adams, P. Lopes, and T. Choudhury, "Affective Touch as Immediate and Passive Wearable Intervention," *Proceedings of the ACM on Interactive, Mobile, Wearable and Ubiquitous Technologies*, vol. 6, no. 4, pp. 1–23, Dec. 2022.

[40] S. He, H. Zeng, M. Xue, G. Huang, C. Yao, and F. Ying, "Affective Stroking: Design Thermal Mid-Air Tactile for Assisting People in Stress Regulation," *Applied Sciences*, vol. 14, no. 20, p. 9494, Jan. 2024.

[41] J. Hosoi, D. Jin, Y. Ban, and S. Warisawa, "FurAir: Non-contact Presentation of Soft Fur Texture by Psuedo-haptics and Mid-air Ultrasound Haptic Feedback," in *SIGGRAPH Asia 2023 Emerging Technologies*. Sydney NSW Australia: ACM, Nov. 2023, pp. 1–2.

[42] ——, "Voluminous fur stroking experience through interactive visuo-haptic model in virtual reality," *IEEE Transactions on Haptics*, vol. 18, no. 1, pp. 232–243, 2025.

[43] C. Shultz and C. Harrison, "LRAir: Non-contact Haptics Using Synthetic Jets," in *2022 IEEE Haptics Symposium (HAPTICS)*, Mar. 2022, pp. 1–6.

[44] W. Moore, J. Nikesjö, O. Bouchatta, A. D. Makdani, P. Hakizimana, M. Rousson, B. Duvernoy, S. McIntyre, L. J. Pehkonen, A. Fridberger, F. McGlone, H. Olausson, S. S. Nagi, and A. Marshall, "Robust coupling between the C-tactile afferent and the hair follicle in humans," *The Journal of Physiology*, vol. 603, no. 16, pp. 4593–4608, 2025.

[45] M. F. Nolan, "Two-point discrimination assessment in the upper limb in young adult men and women," *Physical Therapy*, vol. 62, no. 7, pp. 965–969, July 1982.

[46] G. N. Abramovich, T. A. Girshovich, S. Iu. Krasheninnikov, A. N. Sekundov, and I. P. Smirnova, "The theory of turbulent jets (2nd revised and enlarged edition)," *Moscow Izdatel Nauka*, Jan. 1984.

[47] I. Wygnanski and H. Fiedler, "Some measurements in the self-preserving jet," *Journal of Fluid Mechanics*, vol. 38, no. 3, pp. 577–612, Sept. 1969.

[48] J. Harkki, P. Tuovinen, V. Jousmäki, G. Barreto, P. Rapeli, J. Palomäki, J. Annevirta, A. Puisto, F. McGlone, H. Nieminen, and H. Alho, "Ct-optimal touch modulates alcohol-cue-elicited heart rate variability in alcohol use disorder patients during early abstinence: A randomized controlled study," *Alcohol*, vol. 123, pp. 19–26, 2025.

[49] E. Eriksson Hagberg, R. Ackerley, D. Lundqvist, J. Schneiderman, V. Jousmäki, and J. Wessberg, "Spatio-temporal profile of brain activity during gentle touch investigated with magnetoencephalography," *NeuroImage*, vol. 201, p. 116024, 2019.

[50] S. Lakatos and R. N. Shepard, "Constraints common to apparent motion in visual, tactile, and auditory space." *Journal of Experimental Psychology: Human Perception and Performance*, vol. 23, no. 4, pp. 1050–1060, 1997.